

Vibrational relaxation of OH ($X^2\Pi$, $v=2$)

Karen J. Rensberger, Jay B. Jeffries, and David R. Crosley

Citation: *J. Chem. Phys.* **90**, 2174 (1989); doi: 10.1063/1.456671

View online: <http://dx.doi.org/10.1063/1.456671>

View Table of Contents: <http://jcp.aip.org/resource/1/JCPSA6/v90/i4>

Published by the AIP Publishing LLC.

Additional information on J. Chem. Phys.

Journal Homepage: <http://jcp.aip.org/>

Journal Information: http://jcp.aip.org/about/about_the_journal

Top downloads: http://jcp.aip.org/features/most_downloaded

Information for Authors: <http://jcp.aip.org/authors>

ADVERTISEMENT



nvidia RUN YOUR GPU
CODE 2X FASTER.
TRY A TESLA K20 GPU
ACCELERATOR TODAY.
FREE.

Vibrational relaxation of OH ($X^2\Pi, v=2$)

Karen J. Rensberger, Jay B. Jeffries, and David R. Crosley
Molecular Physics Laboratory, SRI International, Menlo Park, California 94025

(Received 28 September 1988; accepted 2 November 1988)

Vibrational relaxation rates for the $v=2$ level of the $X^2\Pi$ state of the OH radical have been measured in a low pressure flow system, using a novel two-laser pump-and-probe technique. The OH is prepared in the $v=2$ level by overtone pumping ($2\leftarrow 0$) and monitored by ultraviolet laser-induced fluorescence in the (1,2) band of the $A-X$ system. Scanning the time delay between the lasers at a given collider pressure produces exponential decay whose rate as a function of collider pressure yields the rate constant. We determine values (all $\text{cm}^3 \text{s}^{-1}$ units) for NH_3 : $(1.20 \pm 0.15) \times 10^{-10}$; CH_4 : $(2.3 \pm 0.2) \times 10^{-12}$; CO_2 : $(6.7 \pm 1.1) \times 10^{-13}$; N_2O : $(4.6 \pm 0.6) \times 10^{-13}$; O_2 : $(2.6 \pm 0.54) \times 10^{-13}$; N_2 and H_2 : $\leq 10^{-14}$. Except for ammonia, these are two to three orders of magnitude smaller than those measured for relaxation of $v=1$ in the $A^2\Sigma^+$ excited state of OH, where attractive forces appear to play a role.

I. INTRODUCTION

The hydroxyl radical is a species of both practical and theoretical importance. It is a key intermediate in the chemistry of both the atmosphere and combustion. Measurements of its vibrational relaxation rates are important for schemes in which OH is monitored using laser-induced fluorescence (LIF), as well as providing a test of theoretical concepts. OH has a large dipole moment, vibrational frequency, and rotational constant similar to the hydrogen halides. However, as a free radical, it has a much different chemical reactivity than those molecules. The study of OH in the ground state offers the opportunity to investigate the effects of these properties on the vibrational relaxation rates.

Vibrational energy transfer (VET) of ground state diatomic molecules has been the subject of extensive experimental and theoretical study.^{1,2} The rate of energy transfer for the relaxation of hydrogen halides³ by a number of different collision partners appears to correlate with decreasing energy defect. The self-relaxation rates decrease with increasing temperature, behavior typical of systems where attractive forces are dominant. Relaxation for the low vibrational levels is, in general, rather slow, taking many hard sphere collisions for the energy transfer process to occur, but it is much faster than for nonpolar diatomics. A smaller number of measurements have been performed on the relaxation of reactive free radical species; some rate constants are available for OH and NO, in both the excited and ground electronic states. In the excited state, OH undergoes VET in a manner governed by attractive forces and collision complex formation. In its ground state, NO is only slightly polar, but shows the same temperature dependence for self-relaxation as the hydrogen halides, an effect attributed to curve crossing and/or collision complex formation. A study of ground state OH is therefore of particular interest in understanding vibrational relaxation mechanisms.

In this work, we use a two-laser pump-and-probe technique to directly measure vibrational relaxation rate constants for OH ($v=2$) with several colliders. Direct excitation of the first overtone of OH prepares ground state molecules in $v=2$ in a specific rotational state. When combined with laser-induced fluorescence monitoring of the vi-

brationally excited population, this technique provides a straightforward method for obtaining rate constant data. We present here our results for the collision partners NH_3 , CH_4 , CO_2 , N_2O , O_2 , N_2 , and H_2 . We find that the cross section for relaxation by ammonia is very large, 15 \AA^2 , while those for the other partners are much less than 1 \AA^2 . We compare our results to other flow tube studies on OH by Glass *et al.*⁴ and the recent photolysis studies of Cheskis *et al.*⁵; both of these studies require a kinetic model to determine the rate constants. We also compare our results to those previously measured for OH ($A^2\Sigma^+, v=1$), where relaxation cross sections⁶⁻⁹ for all the partners studied here are on the order of 10 to 50 \AA^2 . VET in OH therefore occurs much more slowly in the ground electronic state; in the last section of the paper, we consider this phenomenon and speculate on possible reasons.

II. EXPERIMENTAL METHOD

The apparatus for this study is shown in Fig. 1. It consists of a flow cell in which OH is produced, an infrared laser for direct excitation¹⁰ of ground state OH to a specific rotational level in $v=2$, an ultraviolet laser for probing the OH by laser-induced fluorescence at a variable delay time after the excitation, and the detection optics and electronics.

A trace of hydrogen diluted in helium flows through a microwave discharge to produce H atoms, which react with NO_2 injected in the flow cell above the laser interaction region to generate ground state OH. Calibrated flow meters measure the flows of helium, hydrogen, and a mixture of 1% NO_2 in helium to be typically 3.5, 0.010 and 0.045 ℓ/min , respectively. For some runs, argon is used as the main carrier gas. The background pressure in the flow cell is about 2 Torr. The flow rates of the added collision partner gas, which is added just below the microwave discharge but above the laser interaction region cell to insure adequate mixing, range from a maximum of 1.5 ℓ/min for NH_3 to a maximum of 9 ℓ/min for O_2 . The stated purities of the gases used for collision partners are all at least 99.99% except for CH_4 which is 99.97%. The total pressure measurement together with the mole fractions as measured by the flow meters give the partial pressure of the collision partner gas.

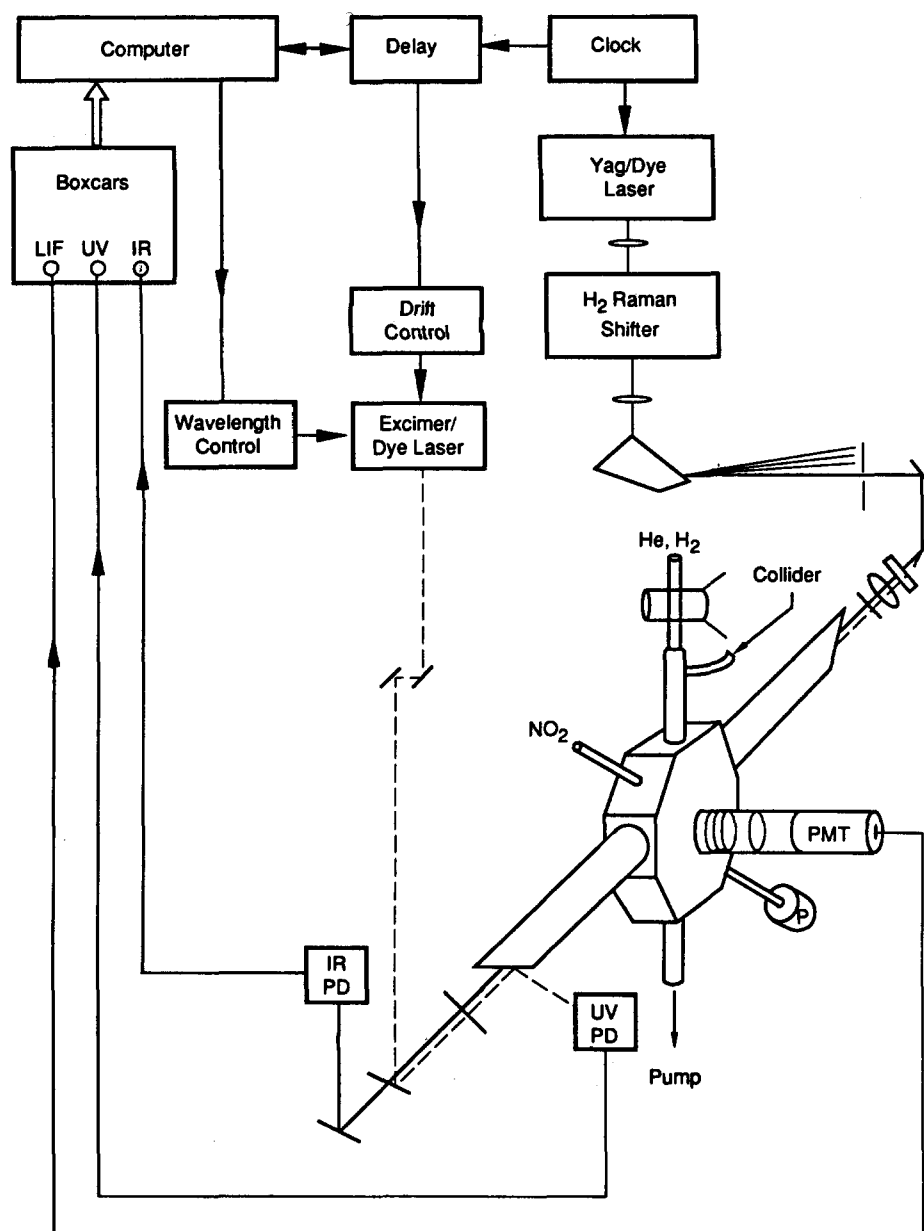


FIG. 1. Schematic of the experimental apparatus.

The second Stokes component of the Raman-shifted output ($\sim 7000 \text{ cm}^{-1}$, 0.9 mJ , $\sim 10 \text{ ns}$, $\sim 0.15 \text{ cm}^{-1}$ bandwidth) of an Nd:YAG laser excited dye laser operating with DCM dye excites a small fraction ($< 1\%$) of the total OH in the flow cell. The excitation is to both λ -doublet components of a specific rotational level in $v = 2$ by either the $R_1(1)$, $Q_1(1)$, or $Q_1(2)$ transition of the first overtone band.^{11,12} Ultraviolet light from an excimer laser excited dye laser operating with BMQ dye dissolved in dioxane (0.3 mJ , $\sim 12 \text{ ns}$, $\sim 0.2 \text{ cm}^{-1}$ bandwidth) probes one of the rotational levels of the OH in $v = 2$ via the $A-X(1,2)$ band $Q_1(1)$ to $Q_1(4)$ transitions near 354 nm .¹³ A 500 mm focal length lens focuses the IR laser beam to a $500 \mu\text{m}$ diameter in the center of the cell; the diameter of the UV beam, which counterpropagates through the cell, is five times larger. The UV beam power is monitored using a photodiode viewing the beam reflected off the cell entrance window. A GG-19 filter blocks the UV laser beam after the cell on the IR entrance side. The

IR beam is transmitted through the UV beam steering mirror and is sent to a power meter. A 6 cm focal length lens collects the fluorescence and focuses it onto a photomultiplier tube, filtered by a combination of a UG-11, GG-19, (Schott) and a solar blind filter (Corion) to eliminate any scattered laser light and emission from the afterglow of the discharge. A boxcar integrator captures the amplified signal, which is then digitized and stored. A computer controlled digital delay generator varies the time delay between the two laser pulses, so that the probe laser measures the direct time dependence of the population in $v = 2$. A drift control box eliminates long term drift which could occur in the time between the excimer laser trigger signal and the actual excimer laser light pulse. The time delay is varied from -4 to $250 \mu\text{s}$ when no collision partner gas is added, where negative values indicate that the UV laser pulse arrives prior to the IR laser pulse in order to obtain a baseline. Under certain flow conditions, there is a small background signal present

when only the UV laser is on due to X -state OH in $v = 2$ remaining from the generation reaction; this is subtracted from the time dependent signal in the analysis. We obtain points at $0.2 \mu\text{s}$ intervals near the location of zero time delay and at intervals from 0.5 to $2 \mu\text{s}$ at longer delays. To avoid problems of long term wavelength drift, we average ten laser shots at each point and vary the delay. After a complete scan of the delay, we then repeat so that a typical data trace consists of 30 to 60 laser shots at each delay value and 100 to 150 different delay values. The signal is normalized by the IR and UV laser pulse intensities as monitored by photodiodes. The laser power levels are sufficiently constant that the normalized signal appears to the eye to be the same as an unnormalized signal.

The probe laser monitors the population in some single rotational level in $v = 2$, which is populated either by the initial excitation of molecules into that level or by rapid rotational energy transfer to some adjacent level following that

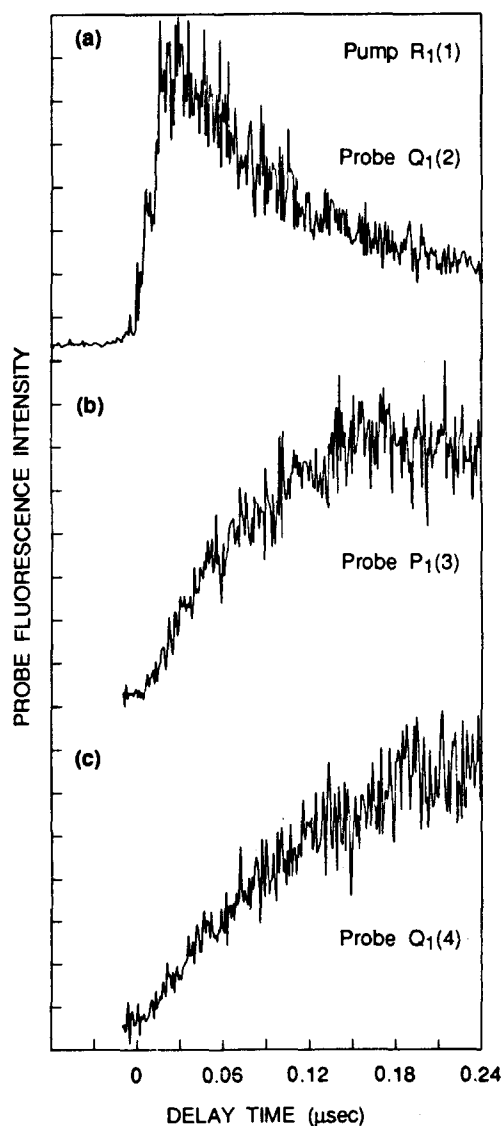


FIG. 2. Time dependence of OH ($X^2\Pi, v = 2$) from 0 to 240 ns in the rotational levels (a) $N = 2$, (b) $N = 3$, and (c) $N = 4$ following excitation to $v = 2, N = 2$. The OH is produced in a water microwave discharge at 0.2 Torr.

excitation. Time-dependent signals obtained when exciting and probing the same rotational level in $v = 2$ show a fast rise and then a slower decay, as shown in Fig. 2(a) for OH produced in a 0.2 Torr microwave discharge of water. The rise time of the signal is about 20 ns, and is determined by the finite pulse width of the excitation and probe lasers and the jitter between the two (~ 8 ns). The peak signal decreases rapidly as molecules are transferred from the initially excited rotational level to neighboring levels. The signal for $N' = 3$ shown in Fig. 2(b) rises faster than that for $N' = 4$ [Fig. 2(c)] after excitation to $N' = 2$. Signal traces from levels one or two rotational levels away from the initially excited level rise to a maximum in less than 500 ns. We have some preliminary data¹⁴ on the rotational relaxation of OH ($v = 2$) by helium, in which equilibration is achieved in less than $5 \mu\text{s}$ at helium pressures of 1.65 Torr. Figure 3 shows the signals obtained on a longer time scale for OH with helium and nitrogen. The upper trace obtained while exciting and probing the same rotational level shows a sharp spike, which is analogous to the signal shown in Fig. 2(a) with an expanded time scale, and then a slow decay due to vibrational relaxation. With no added collision partner gas, vibrational relaxation seen in Fig. 3 is caused by the 2 Torr of background microwave discharge gases, primarily helium, but also any excess hydrogen, H atoms, and reactively produced NO as well as diffusion and directed (pumped) flow out of the probed volume.

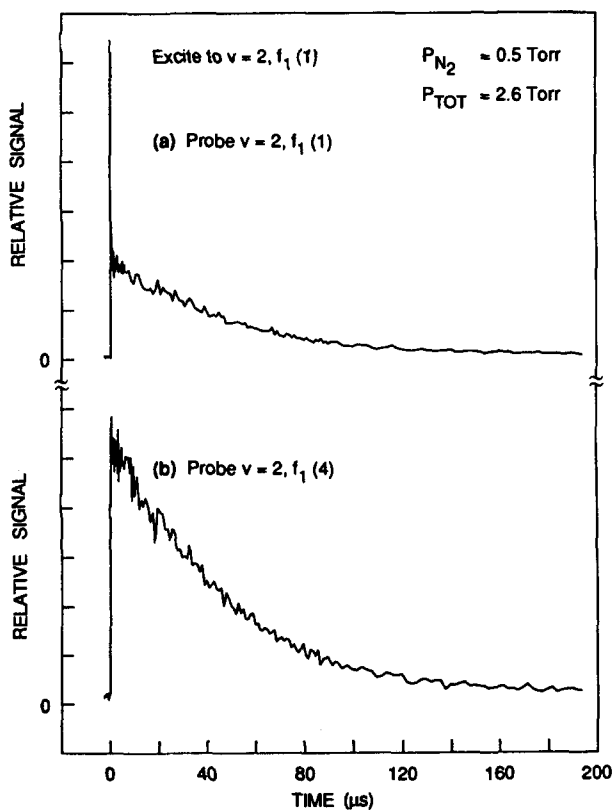


FIG. 3. Time dependence of OH ($X^2\Pi, v = 2$) from 0 to 200 μs in the rotational levels (a) $N = 1$ and (b) $N = 4$ following excitation to $v = 2, N = 1$. The OH is produced by the reaction $\text{H} + \text{NO}_2$ dilute in helium carrier gas. The total pressure is 2.6 Torr including N_2 collider at a partial pressure of 0.5 Torr.

With our flow rates and base pressure of 2 Torr, single exponential signals are obtained when the UV laser probes rotational levels other than the initially excited level, as shown in Fig. 3(b). Care is taken to minimize loss of population in $v = 2$ due to diffusion or flow out of the laser interaction region by using a large UV probe beam size, gas flow velocities less than 300 cm/s, and carrier gas pressures in excess of 1 Torr. Before adding the collision partner gas, we verify that the signals are single exponential. The amount of NO_2 added is minimized until the signal size begins to decrease and then increased 10%. A fit between 90% and 10% of the peak value for signals such as the one shown in Fig. 3(b) yields a decay constant for the removal of OH ($v = 2$). The decay constant is the sum of the radiative rate and the collisional removal rate. The radiative rate for OH ($v = 2$) is very slow, and may be disregarded here.¹¹ The collisional removal rate is the sum of that from the background microwave discharge gases and that from the added collision partner gas.

III. RESULTS

Figure 4 displays the measured decay constants vs partial pressure of added ammonia. The slope of a linear least-squares fit to the data provides the total removal rate constant. The intercept is the contribution of the background gases, mostly helium, to the removal rate. Two sets of data are plotted for NH_3 . The larger data set was acquired early in the experiment, when faster pumping speeds and a smaller UV beam size than discussed above was used. The second set of data was taken with the conditions detailed above. The slopes of the fits to each data set agree to within their statistical error limits, and we report the weighted average of the two slopes. The relaxation rate constant for NH_3 is quite large: $k = (1.20 \pm 0.15) \times 10^{-10} \text{ cm}^3 \text{ s}^{-1}$. The intercepts for the two data sets are quite different, reflecting the change in experimental conditions. For the conditions using a large

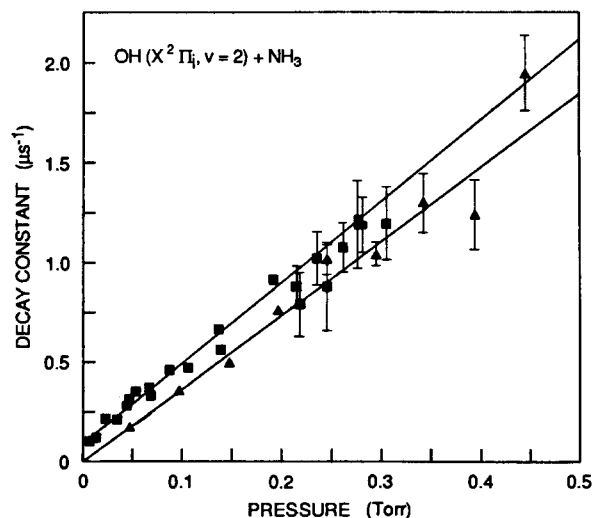


FIG. 4. Pressure dependence of the decay constants for OH ($X^2\Pi_i, v = 2$) with NH_3 . The squares indicate data taken with a smaller probe beam size and higher gas flows than the triangles. The lines are the linear least-squares fits to each data set.

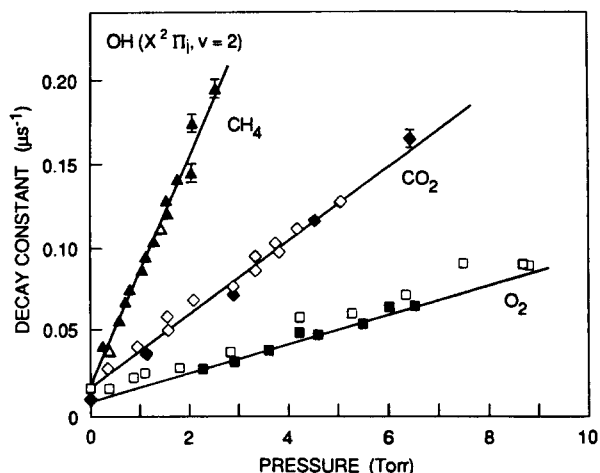


FIG. 5. Pressure dependence of the decay constants for OH ($X^2\Pi_i, v = 2$) with CH_4 , CO_2 , and O_2 . All the O_2 data is with helium as the carrier gas; the open symbols are data taken with the O_2 flowing through a cold trap. For the CH_4 and CO_2 data, the closed and open symbols indicate the use of helium and argon as the carrier gas, respectively.

UV beam, the intercept is typically 0.01 to 0.02 μs^{-1} ; the larger intercept with the smaller UV beam waist presumably is due to diffusion, with minor contributions from directed flow, of the radicals out of the region probed by the UV laser.

Figure 5 shows plots of the measured decay constants vs partial pressure for three of the added gases: CH_4 , CO_2 , and O_2 . The data points for N_2O , which are not shown, lie near those for CO_2 . The rate constants are $(2.3 \pm 0.2) \times 10^{-12} \text{ cm}^3 \text{ s}^{-1}$, $(6.7 \pm 1.1) \times 10^{-13} \text{ cm}^3 \text{ s}^{-1}$, $(4.6 \pm 0.6) \times 10^{-13} \text{ cm}^3 \text{ s}^{-1}$, and $(2.6 \pm 0.4) \times 10^{-13} \text{ cm}^3 \text{ s}^{-1}$ for CH_4 , CO_2 , N_2O , and O_2 , respectively. These four collision partners relax OH much less efficiently than does NH_3 . The error limits include 2- σ statistical errors from the fitting procedure added in quadrature with estimates of uncertainty in the measured gas flows, pressure measurement, and possible diffusive loss from the LIF probed volume. The data shown in Fig. 5 include points acquired while probing different rotational levels in $v = 2$. There is no significant difference for the range of $N' = 1$ to 4, as might be expected in that, in the ground state, rotational thermalization appears to occur more rapidly than does VET. We also used Ar as the background diluent for half of the CO_2 data and for two points of the CH_4 data, and found no differences. O_2 is the slowest collision partner shown here. The open points show data from running the oxygen through a dry ice/ethanol cooled trap to check for any influence on the relaxation from impurities in the gas.

Both vibrational energy transfer and removal by reaction contribute to the rate constants; however, the reaction rate constants at room temperature¹⁵ for the exothermic reactions of OH ($v = 0$) with NH_3 , CH_4 , and N_2O are only $1.6 \times 10^{-13} \text{ cm}^3 \text{ s}^{-1}$, $7.7 \times 10^{-15} \text{ cm}^3 \text{ s}^{-1}$, and $< 2 \times 10^{-16} \text{ cm}^3 \text{ s}^{-1}$, respectively, orders of magnitude smaller than our measured total removal rate constants. Reactions with CO_2 and O_2 are endothermic by 61 and 52 kcal/mol and would be expected to have negligible reaction rates. The influence of vibrational excitation of the OH on its reaction rates with

TABLE I. Vibrational relaxation rates and cross sections.

| Collision partner | Rate constant ^a (cm ³ s ⁻¹) OH(<i>X</i> ² Π, <i>v</i> = 2) | Cross sections(Å ²) | | | | |
|-------------------|--|--|--|--|--|---|
| | | OH(<i>X</i> ² Π, <i>v</i> = 2) | OH(<i>A</i> ² Σ ⁺ , <i>v</i> = 1) | NO(<i>X</i> ² Π, <i>v</i> = 1) | HF(¹ Σ ⁺ , <i>v</i> = 1) ^m | HCl(¹ Σ ⁺ , <i>v</i> = 2) ^m |
| NH ₃ | 1.20 ± 0.15 × 10 ⁻¹⁰ 1.0 ± 0.3 × 10 ^{-10b} 0.8 ± 0.3 × 10 ^{-10c} | 14 12 ^b 9 ^c | 14 ^d | ... | 23 | ... |
| CH ₄ | 2.3 ± 0.2 × 10 ⁻¹² 1.3 ± 0.3 × 10 ^{-12c} | 0.26 0.14 ^c | 46 ^d | 2 × 10 ^{-2 f,g} | 0.2 | 0.5 |
| CO ₂ | 6.7 ± 1.1 × 10 ⁻¹³ | 0.09 | 43 ^d | 5 × 10 ^{-4 f} | 0.6 | 2 |
| N ₂ O | 4.6 ± 0.6 × 10 ⁻¹³ | 0.06 | 47 ^d | 2 × 10 ^{-3 g} | 0.1 | 0.8 |
| O ₂ | 2.6 ± 0.4 × 10 ⁻¹³ | 0.03 | 5 ^c 2 ^j | 4 × 10 ^{-3 h,i,k} | 0.001 | 0.001 |
| N ₂ | < 1 × 10 ⁻¹⁴ | < 0.002 | 36 ^d 29 ^c 20 ^j 23 ⁱ | 1 × 10 ^{-4 f} 2 × 10 ^{-5 k} | 0.003 | 0.001 |
| H ₂ | < 1 × 10 ⁻¹⁴ < 4 × 10 ^{-14c} | < 0.001 < 0.002 ^c | 10 ^j 9 ⁱ | ... | ... | ... |
| Ar | < 1 × 10 ⁻¹⁴ | < 0.002 | 0.4 ⁱ | ... | ... | ... |
| He | < 1 × 10 ⁻¹⁴ | < 0.001 | 0.1 ⁱ | 1 × 10 ^{-5 f} | ... | ... |

^a All uncertainties are 2σ.

^b Reference 5.

^c Reference 4, reanalyzed.

^d Reference 9.

^e Reference 8.

^f John C. Stephenson, *J. Chem. Phys.* **59**, 1523 (1973); **60**, 4289 (1974).

^g C. R. Boxall and J. P. Simons, *Proc. R. Soc. London Ser. A* **328**, 515 (1972).

^h R. P. Fernando and I. W. M. Smith, *J. Chem. Soc. Faraday Trans. 2* **77**, 459 (1981).

ⁱ B. D. Green, G. E. Caledonia, R. E. Murphy, and F. X. Robert, *J. Chem. Phys.* **76**, 2441 (1982).

^j Reference 6.

^k R. E. Murphy, E. T. P. Lee, and A. M. Hart, *J. Chem. Phys.* **63**, 2919 (1975).

^l Reference 7.

^m From the compendium of Ref. 3.

these molecules is unknown, although energy added to the OH bond is not expected to enhance the rate of abstraction reactions. A study by Cannon *et al.*¹⁶ shows that single-quantum excitation of OH does not enhance the exothermic, low activation energy reactions of OH with HBr or HCl. In several older studies, Spencer and Glass^{4,17} report that no enhancement could be detected for reactions of OH (*v* = 1) with H₂, CH₄, and HCl; although HBr does react with OH (*v* = 1) 9 times faster than with OH (*v* = 0). We conclude that the observed removal of OH (*v* = 2) is primarily by vibrational relaxation.

A listing of the rate constants and collision cross sections for the five collision partners studied is contained in Table I. They range over 3 orders of magnitude. We also obtain decay plots when adding N₂, H₂, He, and Ar, and see that each of these collision partners is very inefficient. We estimate an upper limit of the rate constant to be ~10⁻¹⁴ cm³ s⁻¹ for each of these gases.

IV. DISCUSSION

We compare our direct measurements on OH VET to the few previously published measurements on OH (*v* = 2), obtained using other, indirect techniques. Our rate constant

for relaxation by NH₃ agrees within error limits with a recent result by Cheskis *et al.*⁵ In that work, vibrationally excited OH radicals are generated by the photolysis of ozone in the presence of NH₃ and monitored by the temporal profiles of the OH by LIF at various NH₃ pressures. A kinetic model is used to extract the vibrational distribution of OH product and to measure vibrational relaxation rate constants for OH, *v* = 1, 2, and 3, to be, respectively, (2.1 ± 0.3) × 10⁻¹¹, (1.0 ± 0.3) × 10⁻¹⁰, and (3.0 ± 1.0) × 10⁻¹⁰ cm³ s⁻¹ for collisions with NH₃. An extension of their technique to other collision partners will be limited by the amount of relaxation that occurs by ammonia in the photolysis mixture, as it is the fastest relaxer measured to date.

Our relaxation rate constants for NH₃ and CH₄ are about four times greater than those reported by Glass *et al.*⁴ using a discharge flow apparatus and electron paramagnetic resonance spectrometer. However, the kinetic model necessary for the analysis furnishes those results only as a ratio of the rate constants for the added collision partner to the rate constant for relaxation of OH (*v* = 1) by NO, for which an early value from Smith¹⁸ of 1.5 × 10⁻¹¹ cm³ s⁻¹ was used. Smith has remeasured that rate constant¹⁹ and found it to be 3.8 × 10⁻¹¹ cm³ s⁻¹. Multiplying the Glass *et al.* results by a factor of 2.5, obtaining for NH₃ *k* = 8 × 10⁻¹¹ and for CH₄

$k = 1.2 \times 10^{-12} \text{ cm}^3 \text{ s}^{-1}$ brings them into close agreement with ours, now differing by about 35%.

The vibrational relaxation of OH appears to follow most of the same trends as the relaxation of the hydrogen halides HF and HCl. Table I also contains rate constants for these molecules and the same collision partners, taken from Ref. 3. Relaxation of the hydrogen halides often occurs by vibrational-to-vibrational (V-V) energy transfer of one quantum of vibrational excitation into some mode of the collision partner. Any excess energy, the energy defect, goes into rotational and translational degrees of freedom. The efficiency of relaxation increases with a smaller energy defect. The plot of OH ($v = 2$) relaxation rate constant vs energy defect shown in Fig. 6 displays this trend (the rotationless energy defects are calculated from spectroscopic constants).²⁰ The role of long-range attractive forces is evident in that the relaxation by the polar molecule NH₃ is much more efficient than relaxation by CH₄, CO₂, N₂O, and O₂ and appears to be enhanced over what would be predicted from the energy defect by a factor of about 30. Ammonia also relaxes HCl and HF rapidly. From these considerations, we expect that H₂O, another polar molecule with a small energy defect, will also be an efficient relaxer. In a microwave discharge of water vapor, we see evidence for this fast relaxation, but as the gases are partially dissociated to an unknown extent, a quantitative determination of the rate constant using this neat water discharge is not possible. Experiments are in progress to make these measurements under better controlled conditions.²¹

Results for the four collision partners He, Ar, H₂, and N₂ are not shown in Fig. 6, as we could obtain for their rate constants only upper limits. All are quite inefficient at vibrationally relaxing OH ($v = 2$). The rare gases have no internal degrees of freedom so the 3400 cm⁻¹ of OH vibrational energy, for single quantum relaxation from $v = 2$, must be converted into translational energy of the OH and the atom, and/or into rotational energy of the OH. Nonetheless, both He and Ar have rate constants at least three times smaller than predicted by the energy defect correlation among the four molecular colliders in Fig. 6. Hydrogen has a vibrational frequency larger than that of OH, so (for single quantum transfer) V-V transfer to H₂ is endoergic by 760 cm⁻¹. This energy gap is over 3 times the thermal energy available at room temperature, so relaxation by hydrogen should also proceed only by transfer of vibrational energy to translation and rotation. In contrast, relaxation by nitrogen, a process with an energy defect of 1070 cm⁻¹, appears to be unexpectedly slow. The energy defect is similar to that for CO₂ but the rate constant is over 60 times smaller. The cause is not that the vibrational mode is infrared inactive, for relaxation by O₂ is close to the value expected from energy defect considerations. In the case of the hydrogen halides, HCl and HF, relaxation by nitrogen is also slow, with rate constants between 1 and $3 \times 10^{-14} \text{ cm}^3 \text{ s}^{-1}$, although this could be ascribed to the infrared inactive mode of the homonuclear collider, for relaxation of these hydrides by O₂ is also slow $k \leq 1.5 \times 10^{-14} \text{ cm}^3 \text{ s}^{-1}$. It is unclear why nitrogen is such an inefficient relaxer for OH ($v = 2$) in comparison to oxygen.

The vibrational relaxation of another open shell radical,

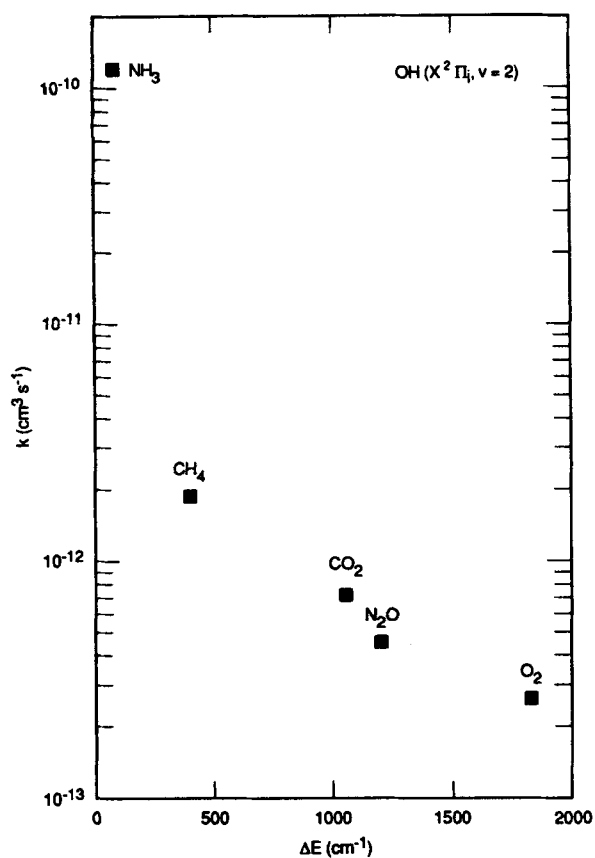


FIG. 6. Plot of the measured rate constant for the relaxation of OH ($X^2\Pi$, $v = 2$) vs rotationless vibration-to-vibration energy transfer energy defect for five collision partners.

NO ($X^2\Pi$, $v = 1$) by the same collision partners investigated here has been studied by several workers. Its relaxation rate constants, also listed in Table I, are an order of magnitude or more smaller than for OH. Further, in contrast to OH, there is no apparent correlation with the V-V energy defect. Self-relaxation for NO appears to occur via a different mechanism, curve crossing or complex formation, but that would not be the case for these colliders. It appears that the open shell, radical nature of these two diatomics does not produce similarities in their vibrational energy transfer.

The pathway by which the ground state OH vibrationally relaxes is not determined in this study, but for NH₃, there is enough transfer to $v = 1$ for LIF detection. We have obtained data for which the UV probe laser is tuned to the $Q_1(2)$ transition of the $A-X(0,1)$ band. The signal as shown in Fig. 7 has a fast rise and a slower fall. The fast rise rate corresponds to the vibrational relaxation rate from $v = 2$, while the slower fall reflects the rate from $v = 1$. After fitting the data with two exponentials, we estimate that the rate from $v = 1$ is at least four times slower than that from $v = 2$. Because of the effects of diffusion out of the laser interaction region, in this preliminary examination, only an upper limit can be obtained. This is significantly different from the ratio of two given by simple theories of VET. The relative fraction of molecules relaxing from $v = 2$ into $v = 1$ could be obtained from the amplitude of signals such as those seen in Fig. 7. One would need to account for possible differences in

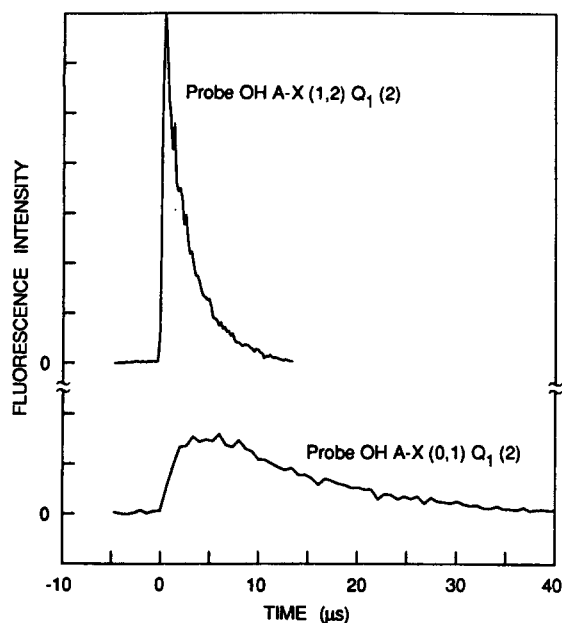


FIG. 7. Time dependence of OH ($X^2\Pi$) in (a) $v = 2, N = 2$ and (b) $v = 1, N = 2$ following excitation to $v = 2, N = 1$ at a total pressure of 1.1 Torr with an NH_3 partial pressure of 0.05 Torr.

upper state fluorescence quantum yields as well as detection efficiencies and probe transition line strengths to determine relative populations and hence the LIF should be performed exciting the same upper state level, i.e., via the (1,2) and (1,1) bands, avoiding different levels of optical saturation in one channel. Such experiments will be performed in the future.²¹ The remainder that do not go into $v = 1$ are molecules which react or relax by a multiquantum transition into $v = 0$.

V. THE ELECTRONIC STATE DEPENDENCE OF VIBRATIONAL ENERGY TRANSFER

The present results, for vibrational relaxation of OH in the $X^2\Pi$, ground electronic state, contrast starkly with those for the $v = 1$ level of the electronically excited $A^2\Sigma^+$ state.⁶⁻⁹ A comparison of our results for $X, v = 2$ and $A, v = 1$ is given in Table I; the excited state cross sections are 10 to 1000 times as large as those for the ground state, for all colliders except NH_3 . In the A state, some collision partners, such as N_2 , are efficient at VET but inefficient at quenching; others (CO_2 , CH_4 , and N_2O) are efficient at both while the polar molecules NH_3 and H_2O are particularly effective quenchers but less efficient at VET, having cross sections for the latter process of some 10 \AA^2 . The large cross sections for both VET and quenching of the A state have been explained by a collision mechanism involving the formation of a transitory complex,^{7,9,22} with the dynamics governed by attractive force interactions in the entrance channel between the OH and the collision partner. A simple multipole interaction picture²² accounts for many of the features of these collisions, and includes forces due to the large dipole moment (2D) of $A^2\Sigma^+ \text{ OH}$.

The $X^2\Pi$, state of OH also has a large dipole moment, 1.7 D, so that one might expect the attractive forces between

the radical and the colliders to be of similar magnitude and thus play a similar role in VET in the two states. Note also that the two internuclear equilibrium distances are nearly the same, and the energy spacings of 3000 cm^{-1} in the A state and 3700 cm^{-1} in the ground state are both large. Behavior governed by attractive forces in both states may be the case for the polar collider NH_3 , whose long-range interactions involve dipole-dipole forces, and which has nearly identical VET cross sections for the two states. However, this is clearly not the case for the other four colliders with cross sections measured here, or N_2 and H_2 for which upper limits were set. In fact, the collision partner for which the rates are most dramatically different is N_2 ; the excited state vibrationally relaxes faster by more than 3 orders of magnitude.

The reason for these differences is thus not apparent. We briefly consider VET in ground and excited states of other diatomics, and then speculate on possible causes of the differences observed in OH.

Rapid vibrational relaxation in excited electronic states of diatomic (and larger) molecules has long been noted.²³ Comparing the $A^2\Sigma^+$ and the $X^2\Pi$ states of NO, Broida and Carrington²⁴ remark that the much faster excited state rate (factors of 20 for CO_2 to 1000 for N_2 , as found here for OH) to be surprising in view of the similarity in the r_e and ω_e values in the two states. Ennen and Ottinger²⁵ compare VET cross sections from a variety of previous measurements for both ground and excited states of several diatomics. To minimize the effects of different collision partners, temperatures and energy defects among the studies in different electronic states, they plot experimental cross sections vs those that they calculated using standard Schwartz-Slowsky-Herzfeld theory.² For all molecules with data available (NO , N_2 , CO , and H_2), the excited state values fall above those for ground states, sometimes dramatically so. Ennen and Ottinger consider the influence of an attractive well depth, assumed to be larger in the excited state due to its larger polarizability. The well depth enters into the SSH formulation in the term $\exp(\epsilon/kT)$, due to the added acceleration before the repulsive part of the curve is encountered. This term is often near unity for ground states, but a large value could explain the size of some excited state cross sections. However, variations in VET for a given molecule and several different colliders do not follow such a pattern. Other suggestions concerning rapid excited state VET have been made because excited states behave like reactive radicals² or that degenerate excited electronic states undergo curve crossings.²⁶ Both appear to be contradicted by the present results where the OH molecule is a radical in both states and the faster upper state is $^2\Sigma$.

As noted, the A and X states of OH have similar geometries and dipole moments, and complex formation seems to explain VET and quenching in the excited state. If this is true, why do complex formation and attractive force interactions not govern VET in the ground state? It is necessary to consider the entire potential for the OH in each state interacting with the collider, not just the attractive part. No such potentials are available for the interaction of OH with the molecular colliders studied here. However, recent LIF experiments²⁷ on OH-Ar van der Waals complexes have fur-

nished potential curves for that molecule. Two important features are evident: First, the total van der Waals well depth in the ground state is one-tenth the 720 cm^{-1} value in the excited state; Second, the repulsive wall occurs at a much larger OH–Ar separation in the ground state. The attractive portions of the curves appear similar, and the smaller well depth in the ground state is apparently due to this earlier onset of repulsion.

We do not know if the potentials for interaction of OH with the molecular colliders studied here show similar features. However, we can speculate concerning the effects on VET of potentials differing between the two electronic states as do those for OH–Ar. Two effects might operate to cause smaller ground state cross sections. First, complex formation will be much less likely in the ground state due to the smaller well depth. Transitory complexes which might form would be much shorter lived, with insufficient time for the OH vibrational energy to be transferred to modes of the complex and ultimately the collider. Second, V–V transfer is known to occur with high efficiency due to attractive interactions such as dipole–dipole and dipole–quadrupole forces.² In the excited state, this mechanism could be operative to mix the vibrational levels. In the ground state, however, the onset of repulsion at larger OH–collider separation may prevent an approach close enough that such attractive forces can be effective. Then, the repulsive wall itself would cause the interaction leading to VET, but it would then occur much less efficiently than if attractive forces were involved.

VI. CONCLUSION

These initial results point to the feasibility of measuring both vibrational and rotational relaxation of OH ($v = 2$), and have provided VET cross sections for several important colliders. Several future experiments are evident. Rotational relaxation including spin–orbit changing and λ -doublet changing collisions will be examined. The inherent simplification of the data analysis resulting from the direct excitation of the OH suggest its extension to pump–probe experiments for higher vibrational levels, to examine the vibrational level dependence of VET. Several vibrational relaxation experiments remain in $v = 2$. A quantitative determination of H₂O relaxation is under way, due both to its importance in atmospheric processes and its fundamental interest. Measurements on the very slow relaxers N₂ and H₂ will be useful for similar reasons, and relaxation by NO might test some ideas of relaxation through complex formation which could include chemical bonding. In addition, a quantitative measurement of the fraction of molecules relaxing in $v = 1$ will be very interesting, and will furnish at the same time the VET rates for that level.

Computation or experiments providing information on the interaction potentials of the OH with these molecular colliders would be valuable, as would trajectory calculations

seeking to identify the mechanism and region on the surface which causes the mixing of the vibrational levels. Of course, VET experiments with collision partners for which surfaces can be calculated, such as He, Ar, or H₂, would clearly be useful.

ACKNOWLEDGMENTS

This work was supported in part by the National Aeronautics and Space Administration and in part by the Air Force Office of Scientific Research.

- ¹J. D. Lambert, *Vibrational and Rotational Relaxation in Gases* (Clarendon, Oxford, 1977).
- ²J. T. Yardley, *Introduction to Molecular Energy Transfer* (Academic, New York, 1980).
- ³S. R. Leone, *J. Phys. Chem. Ref. Data* **11**, 953 (1982).
- ⁴G. P. Glass, H. Endo, and B. K. Chaturvedi, *J. Chem. Phys.* **77**, 5450 (1982).
- ⁵S. G. Cheskis, A. A. Iogansen, P. V. Kulakov, O. M. Sarkisov, and A. A. Titov, *Chem. Phys. Lett.* **143**, 348 (1988).
- ⁶K. R. German, *J. Chem. Phys.* **64**, 4065 (1976).
- ⁷R. K. Lengel and D. R. Crosley, *J. Chem. Phys.* **68**, 5309 (1978).
- ⁸J. Burris, J. J. Butler, T. J. McGee, and W. S. Heaps, *Chem. Phys.* **124**, 251 (1988).
- ⁹R. A. Copeland, M. L. Wise, and D. R. Crosley, *J. Phys. Chem.* **92**, 5710 (1988).
- ¹⁰R. A. Copeland and D. R. Crosley, *J. Chem. Phys.* **81**, 6400 (1984).
- ¹¹S. R. Langhoff, H.-J. Werner, and P. Rosmus, *J. Mol. Spectrosc.* **118**, 507 (1986).
- ¹²J. P. Maillard, J. Chauville, and A. W. Mantz, *J. Mol. Spectrosc.* **63**, 120 (1976).
- ¹³G. H. Dieke and H. M. Crosswhite, *J. Quant. Spectrosc. Radiat. Transfer* **2**, 97 (1962).
- ¹⁴D. R. Crosley, K. J. Rensberger, and J. B. Jeffries, *Bull. Am. Phys. Soc.* **33**, 1629 (1988).
- ¹⁵W. B. DeMore, M. J. Molina, S. P. Sander, R. F. Hampson, M. J. Kurylo, D. M. Golden, C. J. Howard, and A. R. Ravishankara, *Chemical Kinetics and Photochemical Data for Use in Stratospheric Modeling*, Evaluation No. 8, JPL Publication 87-41, 1987.
- ¹⁶B. D. Cannon, J. S. Robertshaw, I.W.M. Smith, and M. D. Williams, *Chem. Phys. Lett.* **105**, 380 (1984).
- ¹⁷J. E. Spencer, H. Endo, and G. P. Glass, 16th Combustion Symposium, 1975, p. 829; J. E. Spencer and G. P. Glass, *Int. J. Chem. Kinet.* **11**, 97 (1977); **9**, 111 (1977).
- ¹⁸D. H. Jaffer and I.W.M. Smith, *Faraday Discuss. Chem. Soc.* **67**, 212 (1979).
- ¹⁹I. W. M. Smith and M. D. Williams, *J. Chem. Soc. Faraday Trans. 2* **81**, 1849 (1985).
- ²⁰G. Herzberg, *Electronic Spectra and Electronic Structure of Polyatomic Molecules* (Van Nostrand, Princeton, 1966); *Spectra of Diatomic Molecules* (Van Nostrand, Princeton, 1950).
- ²¹G. R. Raiche, K. J. Rensberger, J. B. Jeffries, and D. R. Crosley, *J. Chem. Phys.* (to be published).
- ²²P. W. Fairchild, G. P. Smith, and D. R. Crosley, *J. Chem. Phys.* **79**, 1795 (1983); R. A. Copeland, M. J. Dyer, and D. R. Crosley, *ibid.* **82**, 4022 (1985).
- ²³V. N. Kondrat'ev, *Chemical Kinetics of Gas Reactions* (Pergamon, Oxford, 1964).
- ²⁴H. P. Broida and T. Carrington, *J. Chem. Phys.* **38**, 136 (1961).
- ²⁵G. Ennen and Ch. Ottinger, *Chem. Phys.* **3**, 404 (1974).
- ²⁶E. E. Nikitin and S. Ya. Umanski, *Faraday Discuss. Chem. Soc.* **53**, 7 (1972).
- ²⁷M. T. Berry, M. R. Brustein, and M. I. Lester, *Chem. Phys. Lett.* **153**, 17 (1988).